ChemPubSoc Europe

DOI: 10.1002/cctc.201901097

CHEMCATCHEM Full Papers

Mechanism and Control of the Palladium-Catalyzed Alkoxycarbonylation of Oleochemicals from Sustainable Sources

Froze Jameel,[a] Emilija Kohls,[a] and Matthias Stein*[a]

The transformation of chemical production processes to a sustainable feedstock from renewable sources requires a careful assessment of current thermodynamic data, reaction mechanisms and kinetics. The Pd-catalyzed alkoxycarbonylation of the long chain olefin methyl 10-undecenoate (10-UME) from castor oil with methanol yields the building blocks for a renewable polyamide. The mechanism for the complex multi-step reaction cycle including active catalyst formation was elucidated. The experimental catalyst selectivity with 1,2-bis(di-tert-butylphosphino-methyl)benzene (1,2-DTBPMB) as a ligand towards the desired linear diester product can be reproduced and rationalized. The mechanisms of possible side reactions and well as catalyst inhibition by carbon monoxide were also investigated. Solvent effects have an influence on reaction equilibria and transition barriers. These were considered in polar (methanol) and nonpolar (dodecane) media using implicit or mixed cluster/continuum solvation models when explicit solvent coordination was critical.

Introduction

A green chemistry approach towards the synthesis of high-value fine chemicals from renewable feedstock instead of fast depleting fossil resources is becoming an urgent issue in industrial applications. Sourcing and producing responsibly is a challenge to the catalysis and process design at the same time. It would be beneficial if the existing production lines would continue to be in operation with feedstock or intermediates obtained from renewable resources.[1]

Hydroesterification (HE) also known as alkoxycarbonylation, discovered by Walther Reppe in 1953, is the transition metal catalyzed homogenous transformation of an olefin in a reactions with an alcohol (here methanol (MeOH)) and carbon monoxide (CO) to form methyl esters (see Scheme 1).[2] Esters represent an important class of fine chemicals with a wide range of applications in polymer, pharmaceutical, coating, cosmetics and food industries. A constant increase in the worldwide demand of esters has been seen in the last decades; the hydroesterification of ethene has been extensively studied to synthesize of methyl propionate.[3] Over 100 kt of methyl propionate are being produced by the hydroesterification of ethene every year.[4]

[a] F. Jameel, E. Kohls, Dr. M. Stein
Max Planck Institute for Dynamics of Complex Technical Systems
Molecular Simulations and Design Group
Sandtorstrasse 1
Magdeburg 39106 (Germany)
E-mail: matthias.stein@mpi-magdeburg.mpg.de

Supporting information for this article is available on the WWW under https://doi.org/10.1002/cctc.201901097

The transformation of oleochemicals from sustainable sources into long chain esters is of particular interest to the industry.[5] Unsaturated oleochemicals obtained from sustainable resources have proven to be attractive substitutes for fossil fuel-based substrates in the transition metal catalyzed hydroesterification[4,6] producing esters, which are then used as building blocks in the synthesis of the sustainable polyesters and polyamides.[6b]

Since the discovery of the reaction more than sixty years ago, several catalysts have been proposed and tested to achieve high yield and conversion and product selectivity. Drastic reaction conditions (280 °C and 200 bar) were needed to carry out hydroesterification at the beginning. Terminal esters with least amount of isomeric products are highly demanded by industry. Transition metals such as nickel, rhodium, iridium, cobalt, ruthenium, platinum and palladium have been used over time. Palladium catalysts are at least an order of magnitude more reactive than their Pt counterparts.

The geometric and electronic properties of the ligand play an important role in determining the selectivity of the reaction. Bulky bidentate alkyl phosphine ligands are recommended for alkoxycarbonylation.[7] Hydroesterification using different ligands was studied by Gaide et al.[6c] Among the tested ligands, XANTphos gives the high conversion rates. However, the selectivity towards the desired products is low.[4] A high selectivity of 96:4 towards terminal esters was obtained with a palladium catalyst with the electron rich bidentate phosphine ligand 1,2-bis(di-tert-butylphosphino-methyl)benzene (DTBPMB) and methanesulfonic acid (MSA) as a co-catalyst.[4,8] This catalyst system was also found to be very reactive towards both terminal and internal olefins.

From a sustainability and economic point of view, catalyst recovery and reuse are critical. High yields of the linear diester dimethyl dodecanedioate with very low catalyst leaching into the product could be obtained using a thermomorphic solvent

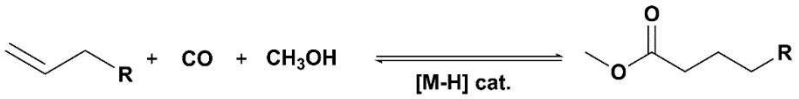

Scheme 1. Production of long chain methoxy ester from unsaturated olefins via hydroesterification.

system (TMS).[4] The TMS exploits a temperature-dependent miscibility gap of two polar and non-polar solvents. At reaction temperature they form a homogeneous phase without any mass transfer limitations during the reaction. Post-reaction reduction of temperature results in a two-component solvent system with a polar catalyst-rich and a nonpolar product-rich phases.

A thorough knowledge of the reaction mechanism, its kinetics and control of both is critical for process development and optimization in the chemical[9] and pharmaceutical industries.[10] Especially the computation of reaction thermodynamics and the microkinetics of each step are key ingredients to rationalize a process and understand chemical reactivity. But also the role of solvent on thermodynamic and kinetic parameters is challenging due to the difficulty with current solvation models.

For the hydroesterification, two possible mechanisms involving either carboalkoxy palladium or hydro-palladium species were discussed.[11] The alkoxy mechanism starts with the formation of a Pd-alkoxy complex, from which by insertion of carbon monoxide the alkoxycarbonyl intermediate is obtained. Olefin coordination and subsequent insertion into the palladium-carbonyl bond form a stable intermediate. Finally, the active catalyst is regenerated by addition of methanol and the elimination of products. The hydride mechanism involves olefin insertion into a palladium-hydride bond, followed by CO insertion into the palladium-alkyl species resulting in a Pd-acyl complex and is completed with the release of the desired ester after alcoholysis (reaction with a methanol solvent molecule), thus regenerating the catalyst (Scheme 2).

It is now commonly agreed that the hydride mechanism is present and solvolysis is rate determining.[8] This information stems from studies with deuterium labelled methanol[12] detailed investigation of the formation of a Pd(II)-hydride catalyst.[3c,d] The role of an acid as a co-catalyst is to generate and stabilize the active Pd(II)–H^+ catalyst. In addition, it preserves catalytic activity by facilitating protonation of catalytically inactive Pd^0 species to regenerate the active Pd(II)–H^+ complex.[3c] Methanesulfonic acid (MSA) was found to be the best co-catalyst in terms of reaction rate and gave the highest yield. Too low amounts of co-catalyst will lead to the formation of palladium black and loss of the activity of the catalyst.[4]

Methanol plays three different roles in the catalytic process. First, it takes part in the reaction as a reagent to form methoxy esters, second it is required to form the active catalyst species, and third, it coordinates to the Pd(II)-hydride complex by occupying the vacant coordination site.[3c]

The coordinated ligand has a fine-tuning effect on the electronic properties of the palladium metal but also its steric demand controls reactivity and selectivity. Methanolysis of linear acyl complexes was found to be favored over that of branched acyl species by sterically demanding ligands decreas-

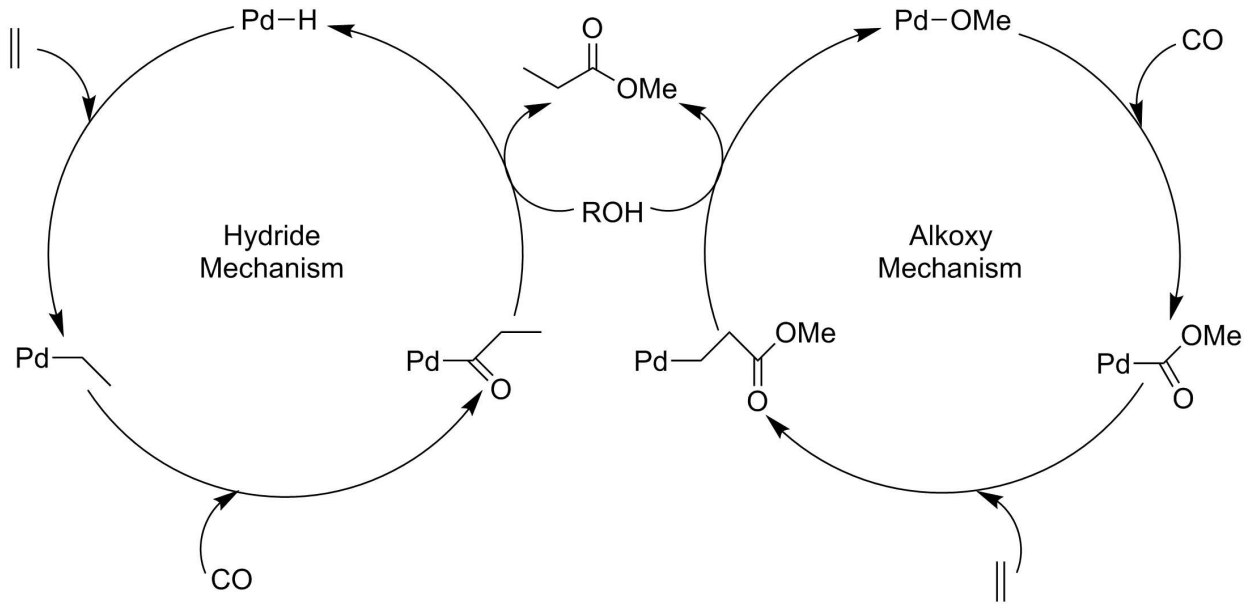

Scheme 2. Simplified hydride and alkoxy mechanisms for the hydroesterification reaction.

ing the activation barrier in this reaction step.[6d,13] Mechanistic studies of alkoxycarbonylation on a model system of palladium catalysis and a short chain olefin suggested methanolysis to proceed via an intramolecular attack of methanol.[6e]

Previous mechanistic quantum chemical studies revealed structural insight into transition states and intermediates of the reaction cycle but were not considering the effect of solvent and solvent coordination sufficiently. The choice of solvent and its influence on the thermodynamics and kinetics has not been studied up to date and will be addressed here in detail.

The hydroesterification of 1-decene with methanol to give methyl 10-undecenoate (UME) was investigated by Gerlach et al. and a kinetic network model was suggested based on three elementary reactions of the cycle. In the presence of CO, isomerization rate was significantly inhibited and high product yields of desired esters could only be achieved at high temperature and low CO pressure.[14] However a more elaborate and detailed mechanistic kinetic model is required to allow process control and optimization which can only be derived after a detailed study of all the reaction steps plus side reactions of the catalytic cycle.

Here, we present a comprehensive mechanistic picture of the hydroesterification reaction (HE) of methyl 10-undecenoate (10-UME) to give the dimethyl dodecanedioate ester (DME) in a thermomorphic solvent system (TMS).[4]

Apart from the preferred pathway to the linear DME product, alternative pathways to branched side-products and other isomers are fully analyzed. This study aims to provide an insight into all the possible microsteps involved in the hydroesterification reaction cycle. The solvent effects have been studied using a mixed cluster-continuum model with an explicit first solvation shell coordination of solvent molecules which is then embedded in an implicit solvent model. The influence of the different polar and non-polar solvents on the thermodynamics and kinetics of different reaction steps of the HE of long chain oleochemical substrates has never been studied before and allows the development of an accurate kinetic model at realistic conditions. This work eliminates model uncertainties and inconsistencies between kinetic experiments[14] and previous computational studies on different chemical systems.[6d,e]

Computational Details

All calculations were performed using TURBOMOLE v. 7.2 2017.[15] Structure were initially optimized using the BP86[16] GGA functional with an Ahlrichs'triple-ξ valence basis set with polarization functions[17] (def2-TZVP) available in the TURBOMOLE library for all atoms.

Optimized structures were characterized by the calculation of second derivatives to correspond to minima, whereas a single imaginary frequency referred to a transition state. The initial guess for transition states searches were made through relaxed energy scans along the reaction coordinate. To verify the transition states, dynamic reaction coordinate scans (DRC) were done along the reaction coordinate by following the imaginary vibrational mole in both directions to connect the transition state with reactants and products, respectively. Gibbs free energies were calculated at experimental operating conditions of 90° C and 30 bar.

For the linear branching point and isomerization pathways, all chemical structures were further refined using the PBE0[18] hybrid functional with dispersion corrections[19] and Becke-Johnson damping.[20] This functional was shown to give reliable and consistent reaction energies for transition-metal catalyzed reactions (MOR41).[21] Thermal corrections were obtained with PBE0-D3/def2-TZVP. Atomic partial charges given are obtained from a Natural Population Analysis (NPA)[22] of the phase of NBO, in which atomic partial charges are obtained through summation over NAOs.

Single point energies at the gas phase optimized structures were calculated using the conductor like screening model (COSMO). [23] Calculations were performed in methanol as a polar ($\varepsilon = 32.7$) and dodecane ($\varepsilon = 2.0$) as a non-polar solvent. This choice of solvent corresponds to the methanol/dodecane solvent system used in the experiments for the hydroesterification of methyl 10-undecenoate (10-UME).[4] In order to assess the effect of a structural re-optimization in COSMO, intermediates 3n, 4n and 6n were re-optimized using COSMO in polar (methanol) and non-polar (dodecane) solvents. Table S1 and Table S2 of the Supporting Information show that no significant structural differences (less than 0.03 Å for bond distances and less than 0.09° for bond angles) can be noted. Also, the difference in solvation energies between re-optimized and single-point calculations is not significant.

Results and Discussion

Reaction Thermodynamics

Thermodynamics and reaction equilibria are of critical importance when it comes to the simulation of chemical reaction networks and processes. Properties such as reaction enthalpy, Gibbs free energy and solvation energy of an ideal system are often not available in literature but can be obtained computationally and then later can be combined with the other thermodynamic approaches to account for the non-ideality of complex reaction mixtures at process conditions.[24] Quantum chemical calculations of thermodynamic data pose a challenge in terms of accuracy.[9] The PBE0-D3 hybrid density functional was recommended for reliable estimates of thermodynamic equilibrium constants K_f from extensive benchmark studies on closed shell metal organic reactions with >100 atoms.[21,25]

The reaction thermodynamics ΔG_r° of the hydroesterification reaction of methyl 10-undecenoate with carbon monoxide and methanol (Figure 1) were calculated in the gas phase and in methanol and dodecane with an implicit solvent environment (COSMO). The free energy of the reaction at process conditions was -104 kJ/mol. This agrees with the previously calculated Gibbs free energy of -107.8 kJ/mol in the gas phase for the hydroesterification of methyl 6-heptenoate with methanol using B3LYP functional.[6d] By taking solvent effects into account, the energy of reaction changes by more than 10 kJ/mol in methanol (see Table 1) and 3 kJ/mol in non-polar dodecane.

The polar solvent shifts the reaction equilibrium to the product side. The effect of solvation on elementary steps of the reaction will be discussed later.

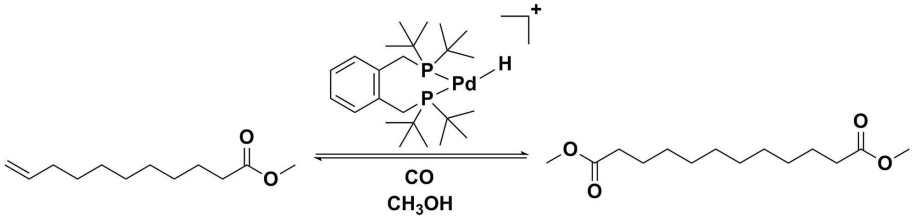

Figure 1. Hydroesterification of methyl 10-undecenoate with a palladium (II) hydride catalyst to give dimethyl dodecanedioate. Ligand: 1,2-DTBPMB.

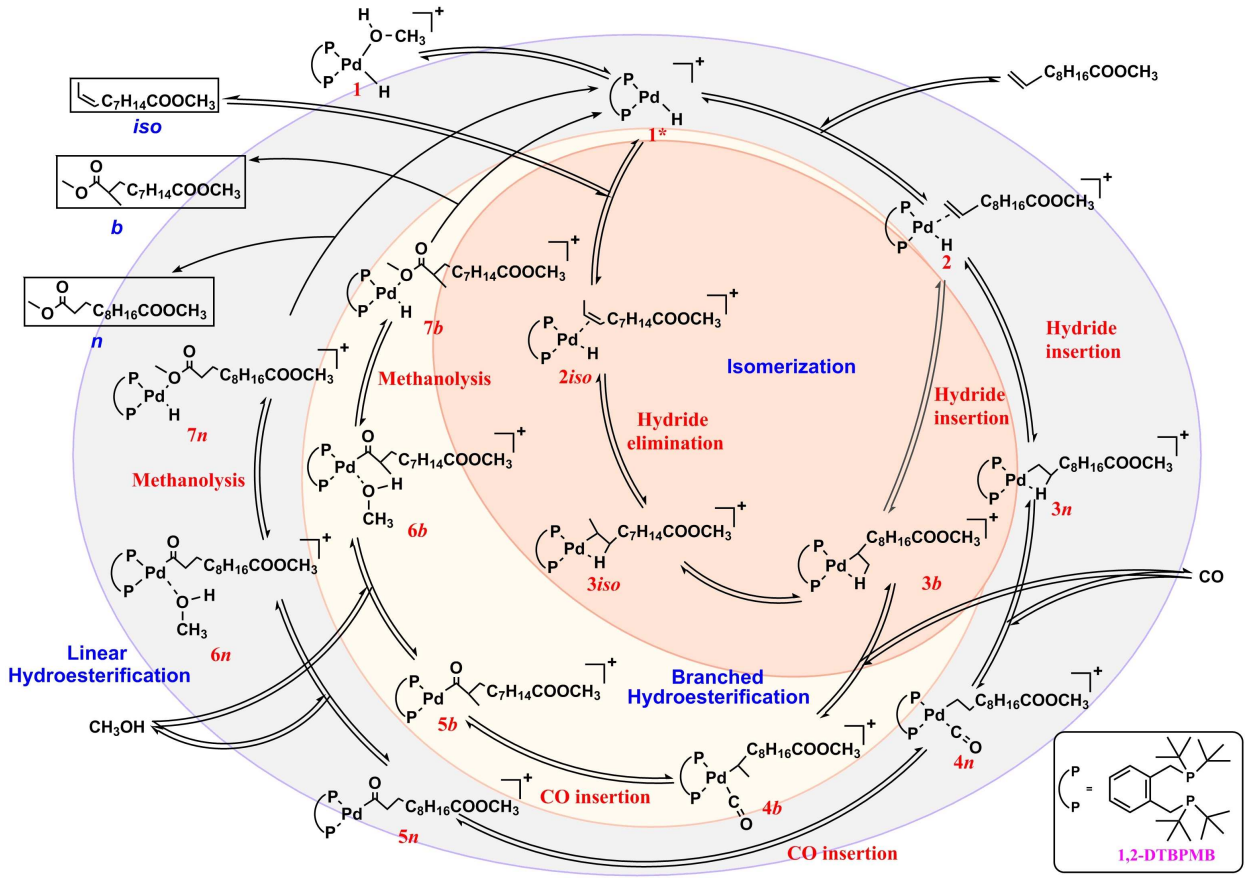

Scheme 3. Catalytic cycle of the synthesis of long chain ester products from oleochemicals by a bidentate phosphine palladium (II) hydride catalyst. All steps, intermediates and transition states connecting them are described and discussed in the text.

Table 1. The Gibbs free energy of reaction (ΔG_r°, in kJ/mol) and solvent effects of the hydroesterification reaction of methyl 10-undecenoate with methanol.

	Free energy of reaction ΔG_r° [kJ/mol]
Gas phase	−104.4
Methanol	−115.0
Dodecane	−108.4

Following the experimental screening,[4] palladium(II) ligated to the electron rich chelating diphosphine 1,2-bis((di-tert-butylphosphino)methyl)benzene [(P P) Pd–H(MeOH)] (P P = 1,2-DTBPMB) was used The active catalyst **1*** [(P P)PdH] is generated after the dissociation of a coordinating methanol solvent molecule from **1**, forming a 16-electron square planer geometry with a vacant coordination site. The presence of methanol was shown to stabilize the precursor.[3c]

Reaction Mechanism

The proposed hydride reaction cycle for the hydroesterification of methyl 10-undecenoate is shown in Scheme 3.

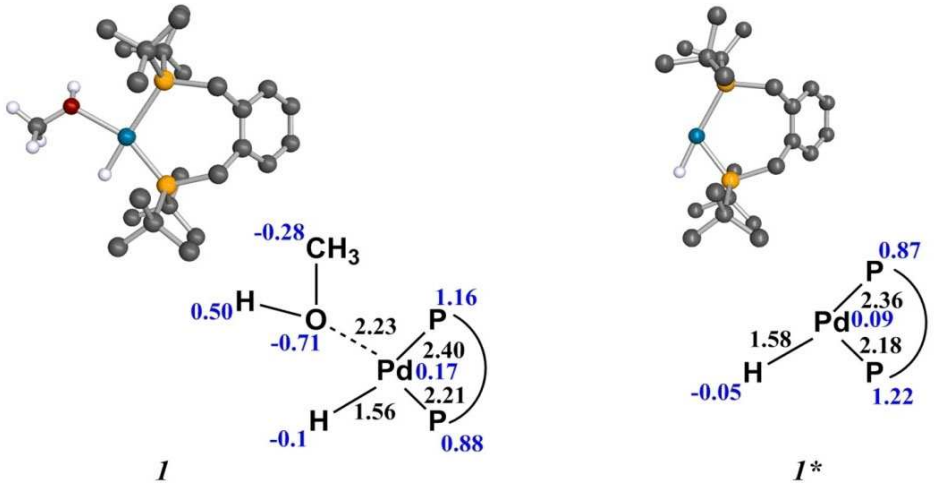

Figure 2. Activation of the pre-catalyst **1** to give the active catalyst **1***. Hydrogen atoms from the ligand were are omitted for clarity. Bond distances (black) are given in Angstroms; NPA charges are given in blue.

Activation of the Pre-Catalyst

The process of the formation of the active catalyst species **1*** HPd(1,2-DTBPMB) from the pre-catalyst **1** has not been addressed before (see Figure 2).

Comprehensive benchmark studies on the WCCR10 set of ligand dissociation energies of large transition metal complexes have shown that dispersion interactions are essential. The PBE0 hybrid functional with dispersion corrections was recommended for accurate calculations of ligand dissociation with results close to DLPNO-CCSD(T) energies.[26]

The energies of methanol dissociation of the pre-catalyst **1** to give the active catalyst species **1*** are given in Table 2.

BP86 without dispersion correction (see Table 2) gives a negative dissociation Gibbs energy of −4 kJ/mol which appears unrealistic. This demonstrates the necessity of inclusion of dispersion effects when calculating realistic binding energies. Addition of D3 corrections gives a methanol dissociation energy of 28 kJ/mol which is only slightly larger than the PBE0-D3 results of 21 kJ/mol. The non-polar dodecane solvent lowers the dissociation energy by 7 kJ/mol, whereas the polar methanol solvent lowers the dissociation energy by 19 kJ/mol to 2 kJ/mol due to the favorable solvation by the released methanol solvent molecule. This shows that at operating conditions, the pre-catalyst **1** and active catalytic species **1*** are in equilibrium and solvent decoordination is facile.

Table 2. Effect of dispersion corrections on the formation of the active organometallic catalytic species **1*** via dissociation of methanol from **1** at 363 K.

Level of theory	Medium	Gibbs free energy ΔG_r° of methanol dissociation [kJ/mol]
BP86	Gas phase	−3.9
BP86 (D3)//BP86	Gas phase	28.0
PBE0 (D3)	Gas phase	21.1
PBE0 (D3)	Methanol	1.9
PBE0 (D3)	Dodecane	13.6

The generation of **1*** is a barrierless process as no transition state could be located along the reaction coordinate which is consistent with all the other studies performed on hydroesterification to date. Besides the effect of an implicit solvation model on the catalyst activation also a hybrid cluster/continuum approach was used. Two explicit methanol molecules form hydrogen bonds with the coordinating methanol molecule in **1**. The active catalyst is generated after dissociation of the coordinated methanol molecule which then form a trimer. The free energy for the catalyst activation with the assistance of explicit methanol molecules was 3 kJ/mol lower than for a single molecule (17.8 kJ/mol compared to 21.1 kJ/mol).

At operating conditions, methanol coordination and dissociation must be considered as a dynamic process and frequent unbinding, re-binding or binding by other solvent methanol molecules may occur.

Substrate Coordination

The substrate methyl 10-undecenoate approaches the catalyst to occupy the vacant equatorial position with the double bond approximately perpendicular to the (P$_\wedge$P)-PdH plane. This results in a distorted square pyramidal geometry. The substrate molecule is slightly unsymmetrically coordinated, which may be attributed to the effects of the long carbon chain of methyl 10-undecenoate, which polarizes the C_α–C_β bond towards the terminal carbon[27] (Figure 3). The Pd–C bond lengths are 2.29/2.36 Å, and they are very close to those reported for the palladium-alkene intermediates.[6e] The C=C bond length in **2** (1.35 Å) is also longer than in the free form (1.32 Å) which indicates the activation of the double bond by the catalyst. The coordination of methyl 10-undecenoate to the catalyst is exergonic by 31.6 kJ/mol. This agrees well with olefin corrdina-

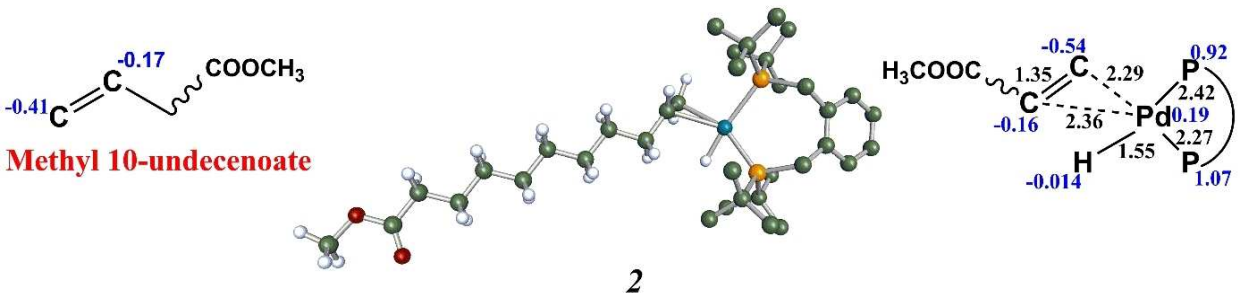

Figure 3. Substrate coordination to the Pd(II) metal center. Hydrogen atoms from the ligand are omitted for clarity. Bond distances (black) are given in Angstroms; NPA charges are given in blue.

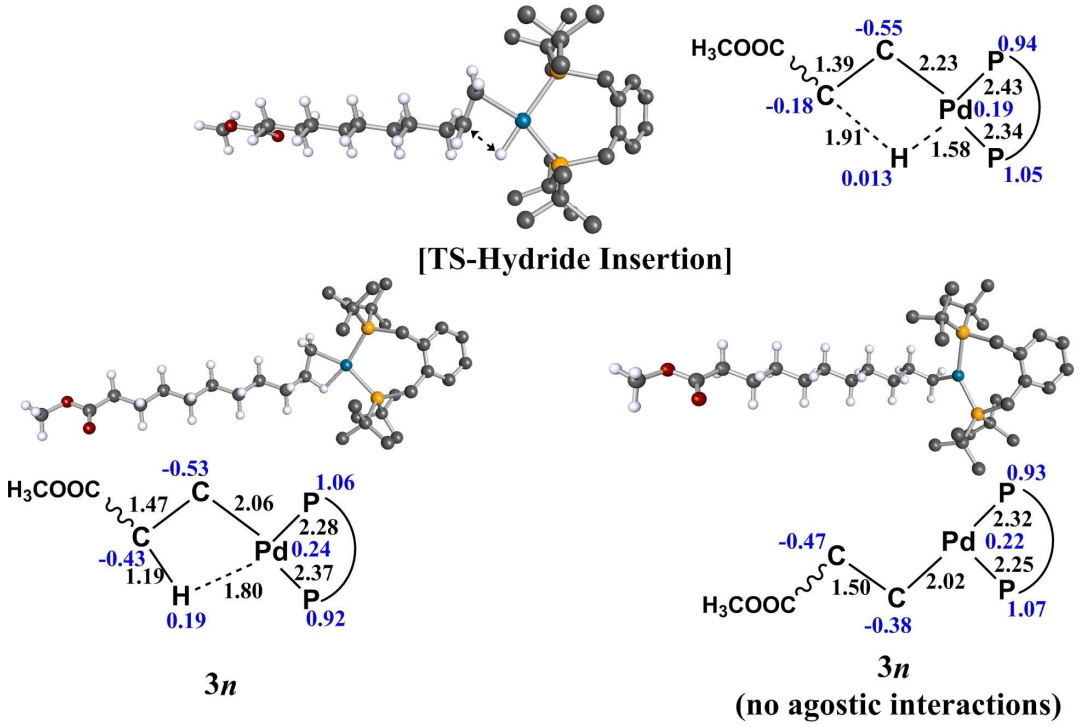

Figure 4. Details of the formation of the Pd-alkyl complex **3n** after the hydride insertion in C–C double bond. Hydrogen atoms from the ligand are omitted for clarity. Bond distances (black) are given in Angstroms; NPA charges are given blue.

tion Gibbs free energy (−41.7 kJ/mol) to the simplified palladium biphosphine catalyst.[6e]

Hydride Insertion

Once the substrate is coordinated to the catalyst, the insertion of the hydride into the UME olefin bond may proceed along two different pathways, resulting in linear and branched alkyl compounds **3*n*** and **3*b*** (Scheme 3), respectively. The metal-alkyl complex is formed passing through a four-center transition state (see Figure 4). A rearrangement of the C=C double bond is necessary for the migratory hydride insertion. At first, the double bond rotates to bring the olefin bond into the Pd–H phosphine plane, followed by the hydride insertion transition state and finally the Pd-alkyl species are obtained. A small activation energy barrier of 1.2 kJ/mol was calculated with BP86 functional (See Supporting Information).

However, for the hybrid functional PBE0-D3 no activation energy barrier could be calculated. This barrierless hydride into the olefin bond and then towards C_β leads to the preferred linear Pd-alkyl complex **3*n*** (see Figure 4). The absence for an energy barrier for the hydride insertion was also reported for B3LYP calculation.[13]

In the Pd-alkyl **3*n***, the complex is stabilized by an agostic (three-center-two-electron) interaction between the metal center and C_β. Agostic interactions play a significant role in the stability and isomerization of Pd-alky complexes. This interaction stabilizes the alkyl complex ***3n*** by 6.26 kJ/mol relative to the complex with a mono-coordinate ligand (see Figure 4). NMR

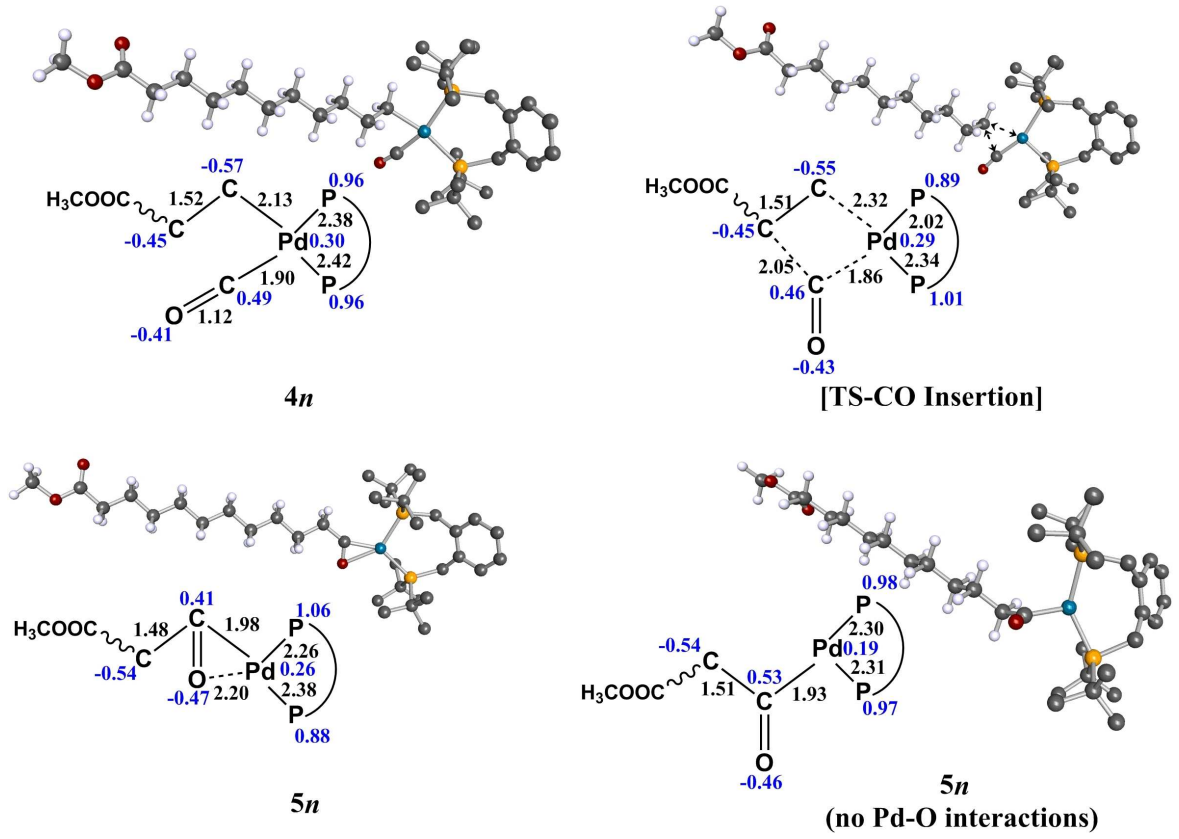

Figure 5. Optimized structures for the CO coordination and insertion steps. Hydrogen atoms from the ligand are omitted for clarity. Bond distances (black) are given in Angstroms; NPA charges are given in blue.

studies have also suggested a β-agostic interaction rather than solvent coordination in ***3n***.[6d] The insertion of the hydride into the olefin bond to give the linear Pd-alkyl complex is thermodynamically favorable by 44.4 kJ/mol (from ***2*** to ***3n***).

CO Coordination and Insertion

The next step in reaction is the carbonylation step, which involves CO coordination to palladium (II) alkyl complex **3*n*** to form **4*n*** and a subsequent insertion of CO into the Pd-alkyl bond, resulting in the Pd-acyl species **5*n***. High temperature and pressure are needed in order to dissolve CO in the reaction mixture.[28] CO occupies the fourth coordination site displacing the agostic interactions and a square-planar structure (**4*n***) is obtained, which is 11.7 kJ/mol higher in Gibbs energy compared to the Pd-alkyl complex **3*n***.

The mechanism of CO insertion into Pd–C bond follows a concerted motion of the alkyl chain towards the carbonyl ligand forming the Pd-acyl complex **5*n***. The transition state has a computed free energy barrier of 13.9 kJ/mol.

Two distinct binding modes of the carbonyl complex could be distinguished (Figure 5). In the first, both the carbonyl carbon and oxygen interact with the palladium atom with distances of 1.98 and 2.20 Å, respectively. In the second, one coordination site remains vacant and only the carbon atoms form a bond with palladium (at a distance of 1.93 Å). The stabilization energy of the first is 18.5 kJ/mol (2.4 kJ/mol of Gibbs energy) which shows an equilibrium between both coordination modes.

Product Release-Methanolysis

In the final step of hydroesterification with methanol, a methoxy group needs to be added to previously formed acyl complex. First, methanol coordinates to metal center (in a binding situation similar to the pre-catalyst **1**) and later undergoes an intramolecular insertion into the Pd-acyl bond forming the diester product and the active catalyst species **1*** is regenerated. Here, the methanol coordination is an endothermic reaction (unlike above) due to the fact that the acyl chain has to rearrange so that methanol can take the fourth coordination site, resulting in a square planer geometry (Figure 6). This rearrangement slightly elongates the catalyst's P–Pd bond from **5n** to **6n**. For less sterically demanding ligands such as Pd/o-$C_2H_4(CH_2PMe_2)_2$, such an elongation might result in a discoordination of the ligand and a deactivation of the catalyst.[6e] However, for 1,2-DTBPMB no significant elongation (only by 0.03 Å) of the Pd–P bonds was found. Gibbs free energy for the binding of a single MeOH molecule to **5*n*** to generate **6*n*** is endergonic by +31 kJ/mol. The calculated

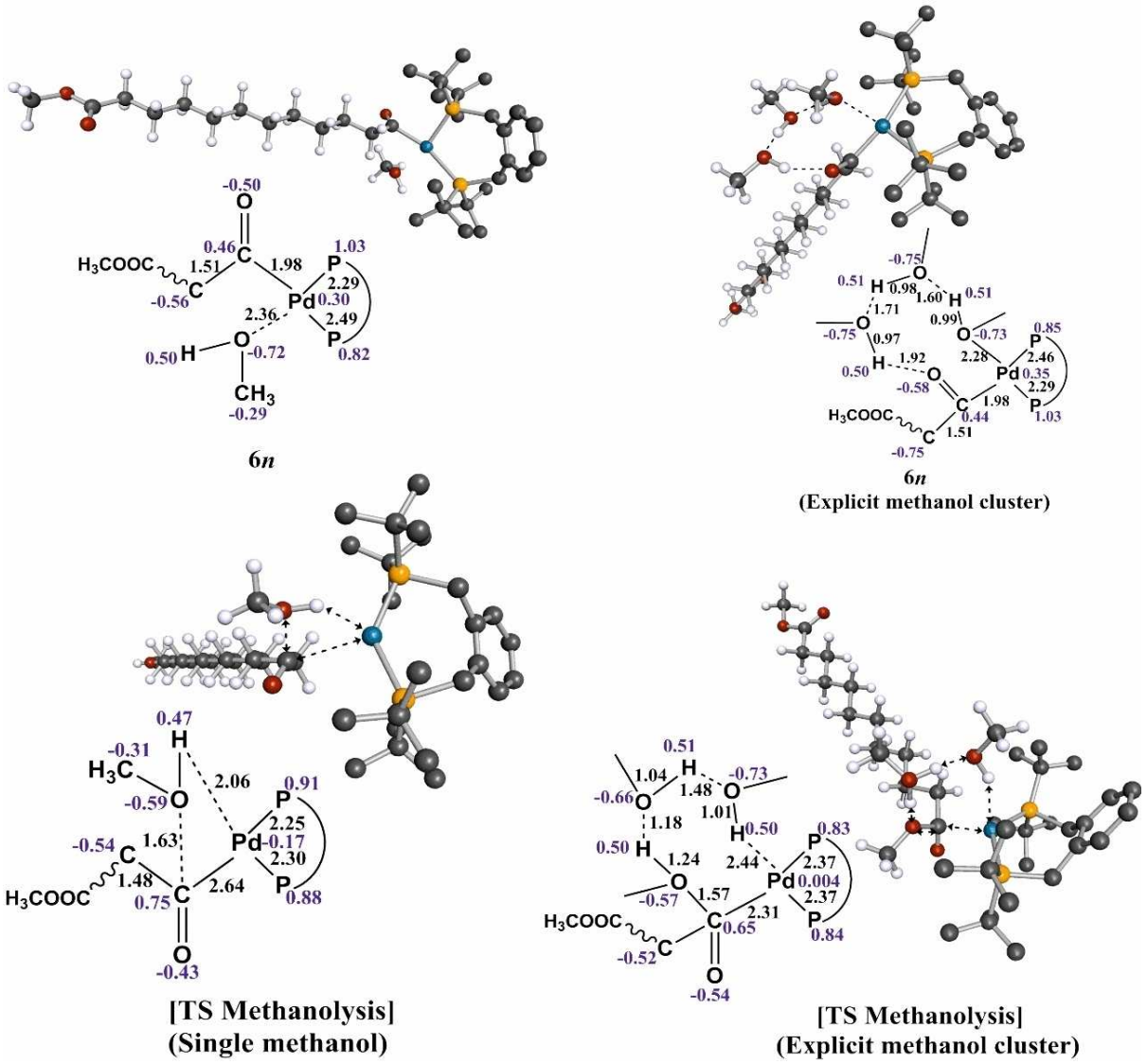

Figure 6. Optimized structures for the stationary points located along the methanol coordination/methanolysis steps. Hydrogen atoms from the ligand were are omitted for clarity. Bond distances (black) are given in Angstroms; NPA charges are given in blue.

activation free energy barrier for methanolysis is 113.7 kJ/mol which agrees very well with a previous value of 121.8 kJ/mol calculated for the methanolysis of methyl 4-heptenoate.[6d]

Explicit solvation models which take into account additional stabilizations by hydrogen bond formations and clustering lower the energy for solvent coordination significantly, for example for the Wacker process coordination of water was significantly enhanced when considering an solvent shell[29] and also for the hydroesterification.[6d] Therefore, we also investigate the final step of methanolysis in a mixed cluster/continuum model with 2 explicitly coordinating methanol solvent molecules (see Figure 6). The cyclic arrangement of these two additional solvent molecules is the optimal coordination geometry to form a network of three hydrogen bonds plus the methanol substrate-Pd interaction. Additional attempts with 2, 4 or more methanol molecules were unsuccessful and did not give stable solvate-solute structures.

The optimized structure **6*n*-3MeOH** shows the formation of three hydrogen bonds between the methanol solvent molecules and the acyl oxygen. The Pd-methanol becomes stronger and the Pd-substrate distance decreases by 0.08 Å whereas the Pd-acyl bond distances is unchanged. The NPA charges show that the formation of a cyclic methanol trimer mediates the Pd-acyl interactions and the positive charge of palladium increases from 0.30 to 0.35 which enhances the methanol binding to Pd. Thus, the unfavorable methanol coordination (+31 kJ/mol) becomes thermodynamically favorable (−3.4 kJ/mol). This compares well the previous value of 31 kJ/mol for the methanolysis of methyl 4-heptenoate.[6d]

Several structural and electronic differences can be observed between the mono- and triple-coordinated methanol-

Pd-acyl complexes. For the three methanol molecules, the Pd-acyl bond length increases by 0.66 Å and the P–Pd–P bite angle increases by 27.6° in the transition states in comparison to the mono-methanol coordinated complex. Such an increase in bite angle might increases the electrophilicity of the acyl moiety and facilitate the formation of a palladium hydride bond.[30,6d]

In the transition state, the electron density at the metal center increases compared to **6*n*** (for a single methanol from 0.30 to −0.17 and for the methanol trimer from 0.35 to 0.004). This increase in the charge density facilitates the final catalyst regeneration.

The explicit solvent methanol molecules form a cyclic ring cluster which enables an efficient concerted proton transfer from methanol to the palladium center to regenerate the hydride. The calculated activation energy of methanolysis in the cluster/continuum model increases by 11.2 kJ/mol (see Figure 7)

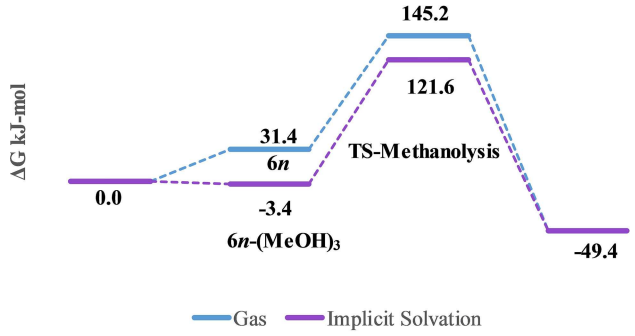

Figure 7. Effect of implicit solvation on the kinetics of methanolysis (rate determining step). Energies are given in kJ/mol relative to the energy of Pd-acyl (**5n**). The energies were calculated at the PBE0-D3/def2-TZVP level.

and similar to the one from Roesle and coworkers.[13] The effect of solvent on the rate determining was studied not only by an implicit but also with hybrid solvation model. No significant effects on the kinetics were observed upon the incorporation of polar and non-polar solvents however the methanol coordination was significantly affected in the polar solvent due to the damping of the electrostatic interaction between the positively charged metal center and the coordinated solvent molecules (see Table 3).

Table 3. Solvent effects on methanolysis of palladium-acyl complex. One substrate methanol *vs.* explicit three methanol molecules coordination embedded in different solvents.

		Gas [kJ/mol]	Methanol [kJ/mol]	Dodecane [kJ/mol]
Single methanol molecule	Thermodynamics of coordination	31.4	48.5	38.0
	Activation energy for methanolysis	113.8	118.8	115.6
Three methanol molecules	Thermodynamics of coordination	−3.4	27.0	8.8
	Activation energy for methanolysis	125.0	116.5	121.8

From these results it can be concluded that explicit methanol coordination facilitates methanol coordination thermodynamically but does not accelerate the final step of methanolysis. The activation energy for methanolysis leading to a branched product (**7*b***) is 131 kJ/mol which is 9.2 kJ/mol higher than for the linear product (see SI for details).

Catalyst Inhibition by Excess CO

In the overall mechanistic picture, the role of CO is crucial since it is both a reactant but also a possible inhibitor of the reaction. It does coordinate to the palladium atom and then forms the acyl complex but it may also inhibit the coordination of other ligands, i.e. substrate and methanol by blocking the coordination site during the reaction. As the reaction is carried out at a pressure of 30 bar of CO, the effect of CO on the reaction elementary steps cannot be neglected. The coordination of CO to active catalyst and the Pd-acyl complex was investigated (Figure 8).

The CO coordinated complexes were found to be thermodynamically stable indicating several possible pathways to deactivation of the catalytic complexes by CO. The calculated free energy for CO coordination to the active catalyst **1*** (−73.5 kJ/mol, see Figure 8) is almost 2.5 times higher than substrate coordination (−31.4 kJ/mol). The rate determining step of methanolysis can also be affected by an excess of CO in the system, as CO inhibits methanol coordination to the Pd acyl complex which was detected in NMR studies.[13] However, there is no firm evidence of the Pd-acyl-CO complex formation to be irreversible or a dead end for the hydroesterification reaction. According to our calculations, coordination of CO to Pd-acyl is almost thermoneutral (0.3 kJ/mol, see Figure 8) therefore we can suggest that the Pd-acyl and Pd-acyl-CO may be in thermodynamic equilibrium. However, CO coordination in comparison to methanol coordination (~31 kJ/mol) to the Pd acyl species, CO coordination is thermodynamically favored. In conclusion, it can be said that an excess of CO drastically effects catalytic activity and might slows down methanolysis by occupying the fourth coordination site. Therefore hydroesterification should be performed at low CO partial pressures. These results are in agreement with experimental finding which reported best yields at the comparatively low CO pressure of 5 bar.[14]

Catalyst Selectivity, Branching Point and Side Reactions

Whereas the linear ester is the desired product, side reactions may lower the overall yield of the production cycle. Olefin coordination (**2**) is the branching point common to all reaction cycles (see Scheme 4). A hydride transfer to C_β leads to **3*n***, the linear product, but hydride insertion into the olefin bond and transfer to C_α leads to the formation branched alkyl species **3*b***. The complete catalytic cycle following the formation of **3*b*** is

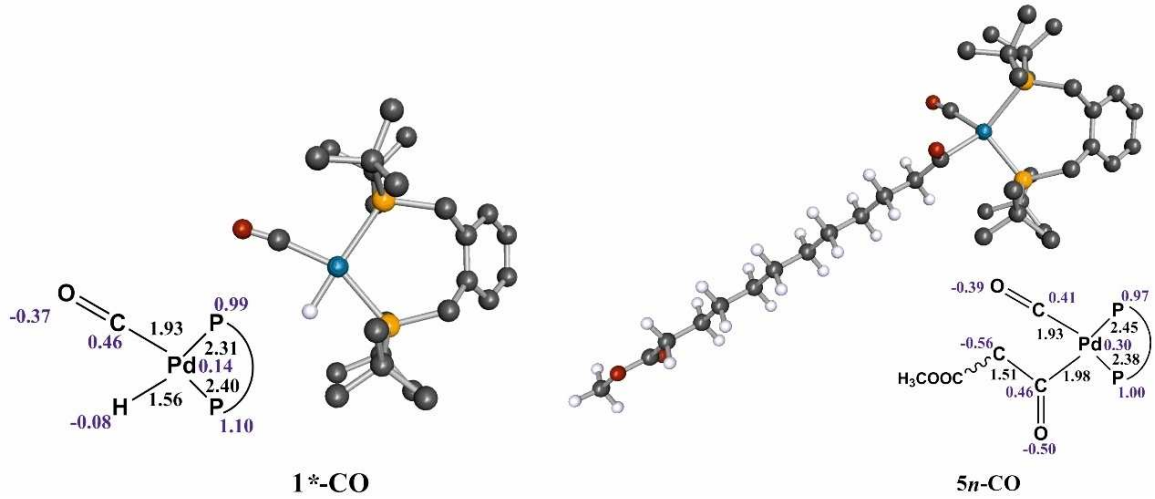

Figure 8. CO coordination to the active catalyst and acyl species hindering the coordination of methanol. Hydrogen atoms from the ligand were are omitted for clarity. Bond distances (black) are given in Angstroms; NPA charges are given in blue.

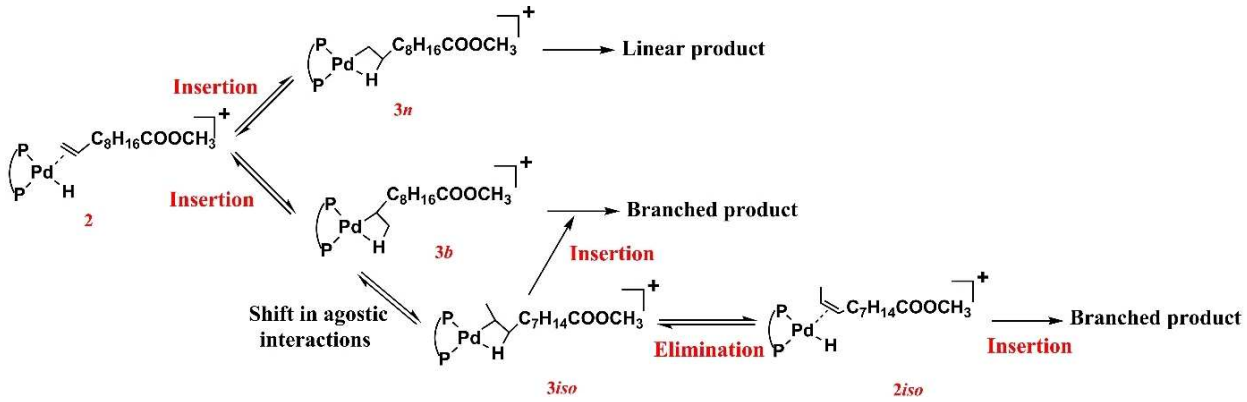

Scheme 4. Hydride insertion branching point and isomerization of substrate lead to the branched products.

given in the Supplementary Information. An ideal catalyst will be able to control the formation of the linear product by suppressing the formation of side products. Figure 9 gives the Gibbs free energy profiles of the first step of the reaction cycle, hydride insertion into the Pd–C bond (from ***2*** to ***3n*** or ***3b***). Formation of ***3n*** is both kinetically and thermodynamically favored and explains the catalyst's selectivity towards the linear pathway.

For the Pd(II) DTBPMB system, the hydride transfer to C_β is a barrierless process while the C_α route has a barrier of +7 kJ/mol. The formation of the alkyl complex **3*n*** is thermodynamically favored over **3*b*** by ~17 kJ/mol.

Assuming that the hydride insertion can be described by a first order reaction, product selectivity can be calculated from an Arrhenius equation. The difference in free energies of activation of the linear *vs.* branched two pathways $\Delta\Delta G^{\ddagger}$ gives the selectivity $S_{lin:branch.}$

We obtain a selectivity $S_{lin:branch}$ of 94:6 for the hydroesterification of UME in methanol, which is in full agreement

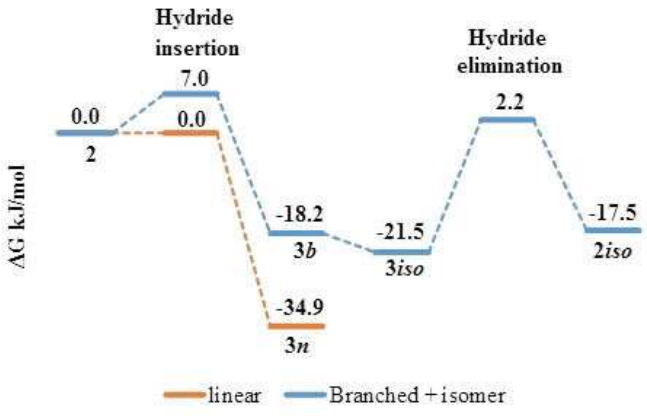

Figure 9. Energy profile (ΔG in kJ/mol) of Cα/Cβ hydride insertion branching point and isomerization along the hydrocarbon chain. The energies were calculated at the PBE0-D3/def2-TZVP level.

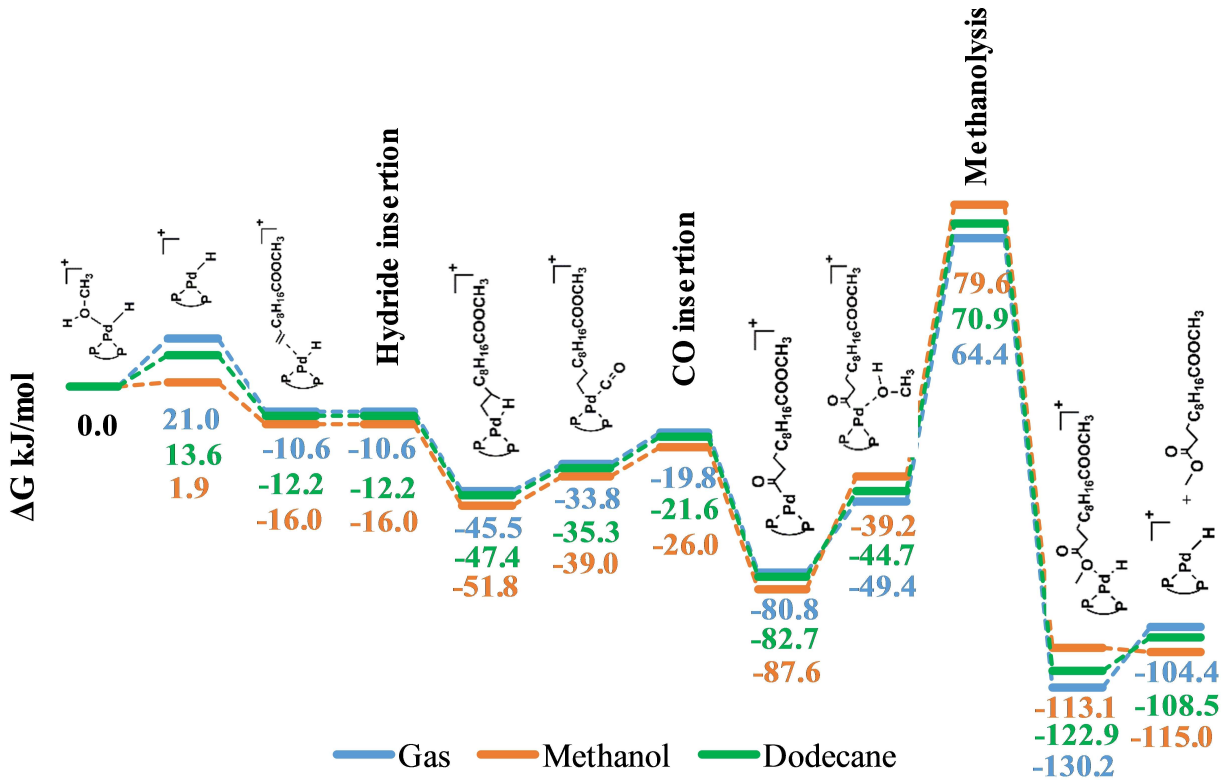

Figure 10. Free energy profile in kJ/mol of the hydroesterification reaction of methyl 10-undecenoate with methanol to give the dimethyl dodecanedioate ester (DME) using the catalyst [(1,2DTBPMB)Pd(II)H(MeOH)],

with the one obtained experimentally for this substrate and catalyst [(1,2-DTBPMB)PdH].[4]

A further side reaction is the double bond isomerization which then may also lead to branched methoxy esters as side products. Bond isomerization proceeds with a C–C bond rotation and coordination of different β-hydrogen atoms to the metal center and then proceeds via a "chain walking" mechanism by a series of β-elimination and insertion reactions (see Scheme 4).

Agostic interactions play an important role in the isomerization of the double bond. Here, we investigate the pathways leading to branched products and isomers of 10-UME. The computed energy barrier for the formation of the branched alkyl complex ***3b*** is +7 kJ/mol (see above).

The double bond of 10-UME can isomerize upon coordination to the palladium catalyst. This involves a shift of the agostic interaction to the next carbon atom (C_β–Pd–C_γ), a hydride elimination from C_γ and formation of a new double bond between C_β and C_γ. The isomerizing shift in agostic interaction is energetically feasible (by 3.3 kJ/mol, see Figure 9) but the activation barrier to the hydride elimination from ***3iso*** to ***2iso*** is almost 3 times higher (23.8 kJ/mol) for the branched alkyl complex than for the formation of **3*b*** from **2** ($\Delta G^{\ddagger} = 7.0$ kJ/mol).

The Gibbs free energy profile in Figure 9 shows that, starting from a terminal C=C in UME, it is energetically unfavorable to follow the branched or isomerization as the linear pathway is clearly favored both kinetically and thermodynamically. This rationalizes the high yield and superior selectivity of this catalyst compared to the experimental findings of Gaide el al.[4]

Gibbs Free Energy Potential Energy Surface

Figure 10 shows the Gibbs free energy profile for entire catalytic cycle of hydroesterification of methyl 10-undecenoate promoted by [HPd(1,2-DTBPMB)] at PBE0-D3/def2-TZVP level of theory in methanol (polar) and dodecane (non-polar) phase. BP86/def2-TZVP results can be found in the SI.

The effect of solvent on the catalytic energy surface was studied using an implicit solvation model. Dodecane as a non-polar solvent has only minor effects on the potential energy surface (PES) and transition state energies. Methanol as the polar constituent of the mixed solvent, however, has a large effect by stabilizing intermediates and lowering transition state barriers. The effects can be as large as 17–19 kJ/mol when stabilizing **1*** and **7*n***. The modifications of the PES occur due to the charge damping effect of the polar solvent. All the microsteps are more favored in the methanol (polar) phase in comparison to the dodecane phase with the exception of methanol coordination and methanolysis. The catalyst activation **1**→**1*** is more favorable in the polar solvent. Dodecane as a non-polar solvent shows a small effects on the energetics of

intermediates and transition state barriers up to step **7*n***. Methanol dissociation energy is reduced from 21 kJ/mol in the gas phase to 1.9 kJ/mol in methanol (see above). Methanol coordination and methanolysis are significantly affected by the inclusion of solvent. The free energy for methanol coordination is higher by 17 kJ/mol in methanol and the activation barrier for the rate determining step of methanolysis increases by 6 and 3 kJ/mol in polar and non-polar solvents, respectively, compared to the gas phase. Similar effects were observed on explicit solvent assisted methanol coordination as the coordination energy was increased by 30.4 kJ/mol (from −3.4 to 27.0 kJ/mol) in the polar solvent. This can only be explained by the strong electrostatic interaction between the Pd(II) and the partially negatively charged oxygen of methanol. The presence of a dielectric medium reduces this interaction depending on the dielectric constant (low or high) and makes them less favorable. The presence of the non-polar solvent, however, facilitates the coordination of three methanol molecules ($\Delta G_{\text{explicit methanol coordination}} = 8.75$ kJ/mol) to the palladium center (see Table 3).

Product dissociation and catalyst regeneration is thermodynamically favored in polar solvent, methanol plays an essential role in catalyst generation and stabilization as discussed above.

In summary, hydroesterification of methyl 10-undecenoate is favored in polar solvent with the exception of methanol coordination. Thus, a carefully balanced TMS of polar and non-polar solvents is not only facilitating product and catalyst separation but also a good compromise regarding reaction equilibria and kinetics.

Experiments have shown that the best conversion of UME is obtained with a 70/30 mixture of methanol and dodecane. This finding can now be corroborated by a careful and detailed investigation of solvent effects on the thermodynamics and kinetics on the hydroesterification. The final microstep, the methanolysis of the acyl complex towards the diester product was found to be the rate determining step with an activation barrier of 79 in polar and 71 kJ/mol in non-polar solvent which agrees well the experimental results for the two-stage methoxycarbonylation of sunflower oil.[6e]

Summary and Conclusions

The use of feedstock from renewable sources requires a detailed analysis of changes in thermodynamics and micro- and macrokinetics of the reaction before it can be transferred and substitute traditional process operations. The full catalytic cycle of the alkoxycarbonylation reaction of methyl 10-undecenoate catalyzed by the organometallic catalyst [(1,2-DTBPMB)HPd(II)] was investigated including side reactions such as isomerization and formation of branched products and CO inhibition. For the first time, the effects of polar and non-polar solvents on every elementary step were analyzed in detail.

Implicit solvent effects were included by means of conductor like screening model (COSMO) but also explicit solvent coordination must be taken into account in a cluster/continuum approach. This study provides new insights which are of interest for both experimental and theoretical communities.

i. According to our calculations, among all the possible routes, the linear pathway is the energetically preferred. This allows to explain the catalyst's selectivity ($S_{lin/branch}$ 94:6) in agreement with the experimental selectivity reported.[4]
ii. Methanolysis from the Pd-acyl complex forming the ester product is the rate determining step. In the absence of any solvent effect, methanol coordination is thermodynamically unfavorable. Only when explicit solvent coordination and stabilization by hydrogen bond formation is taken into account, it becomes feasible. The calculated energy barrier of this rate determining step (80 kJ/mol) is in excellent agreement with experiment (78 kJ/mol).
iii. The solvent effects on the reaction cycle reveal differences between polar and non-polar solvents for different steps. Methanol coordination to the Pd-acyl and methanolysis are favored in non-polar solvent but catalyst activation and product dissociation are significantly stabilized by the polar solvent. This points to an advanced concept of choice of solvent and/or temperature in a TMS system or dosing strategies.
iv. The use of the PBE0 exchange-correlation functional with an appropriate basis set, dispersion corrections and solvation models is able to give reaction energies or differences in free energies in good agreement with experiment. Such accuracy has not been demonstrated before for the alkoxycarbonylation reaction and is also applicable to other transition metal reactions in homogeneous catalysis.

Acknowledgements

This work is part of the collaborative research project (CRC) SFB/TR 63 – Integrated Chemical Processes in Liquid Multiphase System – InPROMPT (project A4). Financial support from the German Science Foundation (DFG) and the Max Planck Society for the Advancement of Science is gratefully acknowledged.

Conflict of Interest

The authors declare no conflict of interest.

Keywords: Homogeneous catalysis · green chemistry · sustainable feedstock · computational chemistry · transition metal catalysis

[1] P. T. Anastas, J. B. Zimmerman, in *Sustainability Science and Engineering, Vol. 1* (Ed.: M. A. Abraham), Elsevier, **2006**, pp. 11–32.
[2] W. Reppe, H. Kröper, *Liebigs Ann. Chem.* **1953**, *582*, 38–71.
[3] a) G. R. Eastham, R. P. Tooze, X. L. Wang, K. Winston. WO 96/19434, 1996; b) W. Clegg, M. R. Elsegood, G. R. Eastham, R. P. Tooze, X. L. Wang, K. Whiston, *Chem. Commun.* **1999**, 1877–1878; c) W. Clegg, G. R. Eastham, M. R. Elsegood, B. T. Heaton, J. A. Iggo, R. P. Tooze, R. Whyman, S. Zacchini, *J. Chem. Soc. Dalton Trans.* **2002**, 3300–3308; d) W. Clegg, G. R. Eastham, M. R. Elsegood, B. T. Heaton, J. A. Iggo, R. P. Tooze, R. Whyman, S. Zacchini, *Organometallics* **2002**, *21*, 1832–1840; e) V.

de la Fuente, M. Waugh, G. R. Eastham, J. A. Iggo, S. Castillón, C. Claver, *Chem. Eur. J.* **2010**, *16*, 6919–6932; f) T. Fanjul, G. Eastham, N. Fey, A. Hamilton, A. G. Orpen, P. G. Pringle, M. Waugh, *Organometallics* **2010**, *29*, 2292–2305.

[4] T. Gaide, A. Behr, A. Arns, F. Benski, A. J. Vorholt, *Chem. Eng. Process.* **2016**, *99*, 197–204.

[5] A. Behr, A. J. Vorholt, in *Organometallics and Renewables* (Eds.: M. A. R. Meier, B. M. Weckhuysen, P. C. A. Bruijnincx), Springer Berlin Heidelberg, Berlin, Heidelberg, **2012**, pp. 103–127.

[6] a) A. Behr, A. J. Vorholt, N. Rentmeister, *Chem. Eng. Sci.* **2013**, *99*, 38–43; b) J. T. Christl, P. Roesle, F. Stempfle, P. Wucher, I. Göttker-Schnetmann, G. Müller, S. Mecking, *Chem. Eur. J.* **2013**, *19*, 17131–17140; c) T. Gaide, A. Behr, M. Terhorst, A. Arns, F. Benski, A. J. Vorholt, *Chem. Ing. Tech.* **2016**, *88*, 158–167; d) P. Roesle, L. Caporaso, M. Schnitte, V. Goldbach, L. Cavallo, S. Mecking, *J. Am. Chem. Soc.* **2014**, *136*, 16871–16881; e) G. Walther, L. R. Knöpke, J. Rabeah, M. P. Chęciński, H. Jiao, U. Bentrup, A. Brückner, A. Martin, A. Köckritz, *J. Catal.* **2013**, *297*, 44–55; f) M. Amézquita-Valencia, G. Achonduh, H. Alper, *J. Org. Chem.* **2015**, *80*, 6419–6424.

[7] E. Drent, P. H. M. Budzelaar, *Chem. Rev.* **1996**, *96*, 663–682.

[8] C. J. Rodriguez, D. F. Foster, G. R. Eastham, D. J. Cole-Hamilton, *Chem. Commun.* **2004**, 1720–1721.

[9] P. Deglmann, A. Schäfer, C. Lennartz, *Int. J. Quantum Chem.* **2015**, *115*, 107–136.

[10] A. Hillisch, N. Heinrich, H. Wild, *ChemMedChem* **2015**, *10*, 1958–1962.

[11] I. del Río, C. Claver, Piet W. N. M. van Leeuwen, *Eur. J. Inorg. Chem.* **2001**, *2001*, 2719–2738.

[12] G. R. Eastham, R. P. Tooze, M. Kilner, D. F. Foster, D. J. Cole-Hamilton, *J. Chem. Soc. Dalton Trans.* **2002**, 1613–1617.

[13] P. Roesle, C. J. Dürr, H. M. Möller, L. Cavallo, L. Caporaso, S. Mecking, *J. Am. Chem. Soc.* **2012**, *134*, 17696–17703.

[14] M. Gerlach, S. Kirschtowski, A. Seidel-Morgenstern, C. Hamel, *Chem. Ing. Tech.* **2018**, *90*, 673–678.

[15] TURBOMOLE v 7.2 2017, a development of University of Karlsruhe and Forschungszentrum Karlsruhe GmbH, 1989–2007, TURBOMOLE GmbH, since 2007; available from http://www.turbomole.com.

[16] a) A. D. Becke, *Phys. Rev. A* **1988**, *38*, 3098–3100; b) J. P. Perdew, *Phys. Rev. B* **1986**, *33*, 8822–8824.

[17] A. Schäfer, C. Huber, R. Ahlrichs, *J. Chem. Phys.* **1994**, *100*, 5829–5835.

[18] a) C. Adamo, V. Barone, *J. Chem. Phys.* **1999**, *110*, 6158–6170; b) M. Ernzerhof, G. E. Scuseria, *J. Chem. Phys.* **1999**, *110*, 5029–5036.

[19] S. Grimme, J. Antony, S. Ehrlich, H. Krieg, *J. Chem. Phys.* **2010**, *132*, 154104.

[20] S. Grimme, S. Ehrlich, L. Goerigk, *J. Comput. Chem.* **2011**, *32*, 1456–1465.

[21] S. Dohm, A. Hansen, M. Steinmetz, S. Grimme, M. P. Checinski, *J. Chem. Theory Comput.* **2018**, *14*, 2596–2608.

[22] A. E. Reed, R. B. Weinstock, F. Weinhold, *J. Chem. Phys.* **1985**, *83*, 735–746.

[23] A. Klamt, G. Schüürmann, *J. Chem. Soc. Perkin Trans. 2* **1993**, 799–805.

[24] M. Lemberg, G. Sadowski, M. Gerlach, E. Kohls, M. Stein, C. Hamel, A. Seidel-Morgenstern, *AIChE J.* **2017**, *63*, 4576–4585.

[25] L. Goerigk, A. Hansen, C. Bauer, S. Ehrlich, A. Najibi, S. Grimme, *Phys. Chem. Chem. Phys.* **2017**, *19*, 32184–32215.

[26] T. Husch, L. Freitag, M. Reiher, *J. Chem. Theory Comput.* **2018**, *14*, 2456–2468.

[27] V. D. Silva, E. N. Dos Santos, E. V. Gusevskaya, W. R. Rocha, *J. Mol. Struct.*, **2007**, *816*, 109–117.

[28] M. Lemberg, G. Sadowski, *J. Chem. Eng. Data* **2016**, *61*, 3317–3325.

[29] P. E. M. Siegbahn, *J. Phys. Chem.* **1996**, *100*, 14672–14680.

[30] E. Zuidema, C. Bo, P. W. N. M. van Leeuwen, *J. Am. Chem. Soc.* **2007**, *129*, 3989–4000.

Manuscript received: June 19, 2019
Revised manuscript received: July 19, 2019
Accepted manuscript online: July 19, 2019
Version of record online: September 4, 2019